

Sensitive Detection of BRCA1 Gene Based on Target Proximity Induced Quenching of the Fluorescence of Copper Nanoclusters

Jing Hu,^a Tong Yang,^a Zhengjia Li,^a Bo Xiao^a and Peng Yu[✉]*,^a

^aSchool of Materials Science and Engineering, Xiangtan University, Xiangtan 411105, China

The mutations of breast cancer susceptibility gene 1 (BRCA1) play an important role in inherited breast cancers. Thus, the sensitive assay of the BRCA1 gene is extremely important for disease diagnosis and human health. Herein, a fast, sensitive and selective assay technique has been constructed based on fluorescent copper nanoclusters (CuNCs). The CuNCs were successfully formed with poly(AT-TA) double stranded DNA (dsDNA) as template. In the absence of the target, a strong red emission was observed under 365 nm ultraviolet (UV) lamp and a big fluorescence response was obtained. However, in the presence of BRCA1 gene, there was only weak red emission and a low response signal was produced because of the target-proximity induced quenching of the fluorescence of CuNCs. The linear range for the BRCA1 gene assay was 2-600 nM, and the limit of detection was 2 nM. The assay technique showed good selectivity, good stability and satisfactory recoveries for the detection of BRCA1 gene in diluted serum samples. Moreover, by integrating a UV lamp and a smartphone, the fluorescence sensor would be transferred to a microfluidic chip, providing a prospective application in point-of-care for monitoring breast cancer risk.

Keywords: breast cancer, gene detection, proximity, copper nanoclusters, fluorescence

Introduction

Breast cancer is the most common malignant tumor in women, with high morbidity and mortality rates. In less developed countries, breast cancer remains the second leading cause of cancer death among women.¹ Therefore, the early screening, diagnosis and treatment of breast cancer have become a growing concern. Positive family history is one of the most important risk factors for developing breast cancer, and approximately 5-10% of all breast cancers have a hereditary background.^{2,3} Most of the breast cancer susceptibility genes are located on human autosomes and can be inherited from parents to offspring by autosomal dominant. Breast cancer susceptibility gene 1 (BRCA1) is one of the most studied susceptibility genes with high penetrance.⁴ More than 80% of inherited breast and ovarian cancers are related to the BRCA1 gene mutations.^{5,6} Therefore, the development of a fast and sensitive deoxyribonucleic acid (DNA) sensor for the detection of BRCA1 gene is extremely important for the disease diagnosis and human health.

Sanger sequencing is considered the gold standard test for BRCA1 detection.⁷ The theoretical limit of detection (LOD) of Sanger sequencing is about 10% of the mutated allele.⁸ In addition, other technologies reported for the analysis of DNA include colorimetry,⁹ electrochemistry,¹⁰ chemiluminescence,¹¹ Raman spectroscopy,¹² laser transmission spectroscopy,¹³ electrochemiluminescence,¹⁴ surface plasmon resonance¹⁵ and fluorescence.¹⁶ Among these methods, the fluorescence method has attracted much attention because of its advantages of simple operation, good selectivity and simple instrument. Culha *et al.*¹⁷ developed a fluorescent sensor based on molecular beacon (MB) probes for the detection of BRCA1 gene. The LOD was estimated to be 70 nM, which was not satisfactory due to the high background noise caused by the MB detection system. Moreover, MB-based fluorescent strategy demanded labor-intensive labeling steps, which increased the sample preparation requirements and the detection cost.

In order to construct the label-free sensors, a great number of nanomaterials have been fabricated for the sensitive detection of BRCA1 gene. Rasheed and Sandhyarani¹⁸ fabricated an electrochemical sensor based on gold nanoparticles (AuNPs) clusters to detect BRCA1 gene. The sensor exhibited excellent sensitivity and selectivity with a LOD of 50 aM target DNA. Borghei *et al.*¹⁹ developed

*e-mail: yupeng@xtu.edu.cn

Editor handled this article: Emanuel Carrilho (Associate)

a label-free detection strategy for the detection of the large deletion mutation in BRCA1 based on DNA-silver nanoclusters (AgNCs) fluorescence. Its LOD was as low as 64 pM. Ju and co-workers²⁰ reported a fluorescence sensor for the detection of single-base mismatch DNA in BRCA1 gene. The developed sensor was based on fluorescence resonance energy transfer (FRET) between quantum dots (QDs) as the donor and AgNCs as the acceptor. Among a wide variety of nanomaterials, DNA-templated copper nanoclusters (CuNCs) are favorable for various applications due to their mild synthetic conditions, good biocompatibility, and abundant and inexpensive precursors.²¹⁻²³ Their formation is derived from the clustering of Cu⁰, which is produced from the chemical reduction of Cu^{II} on DNA backbones. The production of DNA-templated CuNCs is efficient and finished in several minutes under ambient conditions, which endows a substantial basis for their wide applications in versatile nucleic acid-related biochemical analyses.²⁴⁻³¹ Furthermore, the large Stokes shift of DNA-CuNCs is favorable for the relieving of background interference from complex samples, which may provide an opportunity for detection of the analyte from complex biological media.³² Although the breakthrough has been achieved in CuNCs, few works have been reported utilizing the fluorescent CuNCs for the sensitive detection of the BRCA1 gene.

In this work, a sensitive fluorescent sensor based on CuNCs has been fabricated for the detection of BRCA1 gene. As shown in Figure 1, the probe DNA could form the poly(AT-TA) double stranded DNA (dsDNA) with

3'-overhang ends through the inter-molecular hybridization. The poly(AT-TA) dsDNA could template the formation of CuNCs, resulting in a high fluorescence signal for the blank. When BRCA1 gene was present in the reaction system, BRCA1 gene was in close proximity to the dsDNA and hybridized with 3' protruding termini of the dsDNA. As a result, the synthesis efficiency of the CuNCs decreased and the reaction system obtained a low fluorescence signal. The CuNCs were excited at 340 nm and a red-emission was produced at 580 nm. The fluorescence signal of the detection system was inversely proportional to the concentration of BRCA1 gene. The whole detection process could be completed within several minutes due to the fast formation of CuNCs, indicating a promising platform for the fast detection of BRCA1 gene. The stability of CuNCs and the selectivity of the developed fluorescent sensor, as well as the recovery in the serum were also investigated.

Experimental

Chemicals and instruments

All oligonucleotides were synthesized by Shanghai Sangon Biological Engineering Technology & Services Co., Ltd (Shanghai, China) and high-performance liquid chromatography (HPLC)-purified. The 19-mer synthetic, unmodified oligonucleotide related to BRCA1 was used as the target DNA (T-DNA) and its sequence was 5'-GAACAAAAGGAAGAAAATC-3'.³³ Other oligonucleotide sequences were:

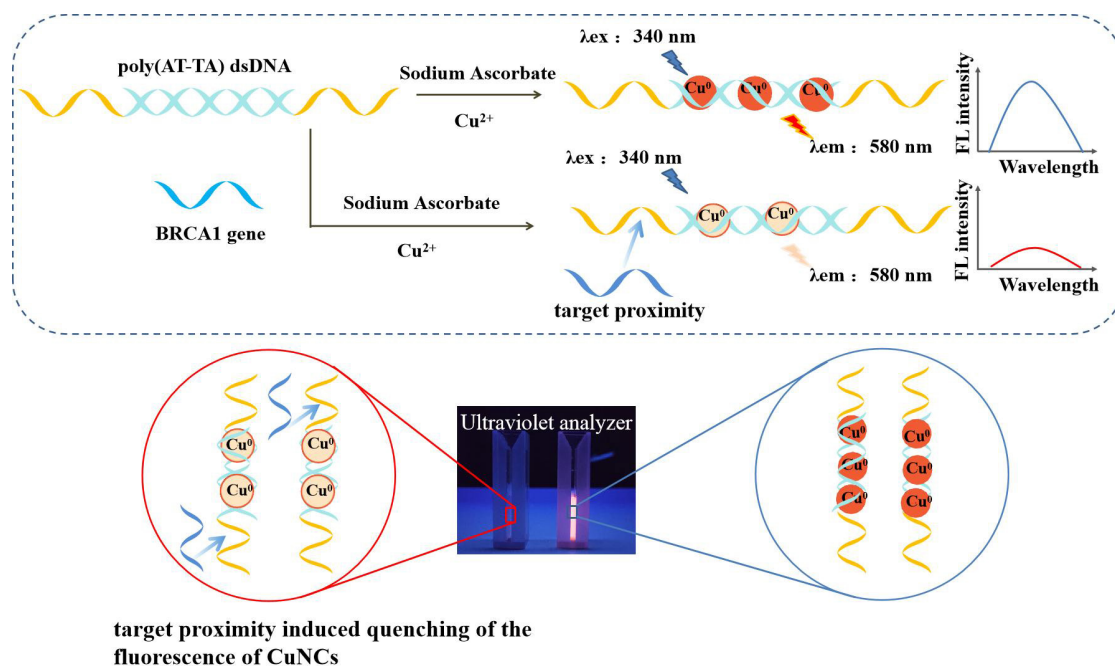


Figure 1. Schematic illustration of the fluorescent sensor based on DNA-CuNCs and its application for the BRCA1 gene assay.

DNA1: 5'-ATCTTCCTTTTGTTC-3';
 DNA2: 5'-ATAATCTTCCTTTTGTTC-3';
 DNA3: 5'-ATATACTTCCTTTTGTTC-3';
 DNA5: 5'-ATA TATATA TCTTCCTTTTGTTC-3';
 DNA7: 5'-ATATATATATATATCTTCCTTTTGTTC-3';
 DNA10: 5'-ATATATATATATATATATACTTCCTTTTGTTC-3';
 DNA13: 5'-ATATATATATATATATATATATATACTTCCTTTTGTTC-3';
 DNA15: 5'-ATATATATATATATATATATATATATACTTCCTTTTGTTC-3';

Single-base mismatched DNA (Sm-DNA): 5'-GAACAAACGGAAGAAAATC-3';

Two-base mismatched DNA (Twm-DNA): 5'-GAACCAAAGGCAGAAAATC-3';

Three-base mismatched DNA (Thm-DNA): 5'-GAACCCACAGGCAGAAAATC-3';

Non-complementary DNA (N-DNA): 5'-CCCCCCCCC
CCCCCCCCC-3'.

3-(*N*-Morpholino)propanesulfonic acid (MOPS), ascorbic acid (AA), copper sulfate pentahydrate, and sodium chloride were purchased from Aladdin-Reagent Company (Shanghai, China). Superior grade fetal bovine serum was bought from Zhejiang Tianhang Biotechnology Co., Ltd. (Zhejiang, China). The fluorescence intensity of the detection system was measured by F-7000 fluorescence spectrophotometer (Hitachi, Japan). All solutions were prepared and diluted with deionized water from a Milli-Q (Bedford, USA) ultrapure water system.

In situ synthesis of CuNCs

The CuNCs were synthesized with the poly(AT-TA) dsDNA as template. 20 μ L of DNA10 (20 μ M), which were placed in a centrifuge tube, were heated in a water bath pot at 90 °C for 10 min and then, cooled at room temperature for 30 min to form the inter-molecular double strands. Then, MOPS buffer (10 mM MOPS, 150 mM NaCl, pH 7.8), 3 μ L CuSO₄ solution (10 mM) and 2 μ L AA solution (100 mM) were added to the centrifuge tube to give a final volume of 100 μ L. Then, the fluorescence signal of the detection system was measured by a fluorescence spectrophotometer. The micrographs of the DNA-templated CuNCs were investigated by high resolution transmission electron microscopy (HRTEM) (JEM-2100, Akishima-shi, Japan).

Fluorescent detection of BRCA1 gene

DNA10 (20 μ L, 20 μ M) and T-DNA were mixed in a centrifuge tube and heated in a water bath pot at 90 °C for

10 min. Then, the mixture was cooled at room temperature for 30 min. After that, MOPS buffer, 3 μ L of CuSO₄ solution (10 mM) and 2 μ L of AA solution (100 mM) were added to the centrifuge tube to give a final volume of 100 μ L. At last, the fluorescence intensity of the detection system was measured using a fluorescence spectrophotometer. For the blank, T-DNA was not added in the detection system, other steps were the same as mentioned above.

Selectivity investigation

A series of oligonucleotides, including Sm-DNA, Twm-DNA, Thm-DNA and N-DNA were used as the interferents for selectivity experiments. The concentration of each interference oligonucleotide and T-DNA was 2000 nM. The fluorescence intensity of the resulting solution was determined by fluorescence spectroscopy at room temperature with excitation at 340 nm.

Results and Discussion

Optimization of the length of poly(AT-TA) in the DNA template

The fluorescence of the DNA-templated CuNCs relied heavily on the sequence composition and sequence length.²³ Although the poly(AT-TA) dsDNA, poly(T) single-stranded DNA (ssDNA) and random dsDNA can be used as templates for the formation of CuNCs, the fluorescence intensity of CuNCs templated by poly(AT-TA) dsDNA was the highest.³² Therefore, the template DNA used in this work was poly(AT-TA) dsDNA and the length of poly(AT-TA) was at first optimized. Several oligonucleotides were chosen as the probe DNA to form the template dsDNA. Then, the template DNA was added in the 100 μ L detection system containing 0.3 mM Cu²⁺ and 2 mM AA to synthesize CuNCs. The lengths of poly(AT-TA) in the different template dsDNA were 1, 2, 3, 5, 7, 10, 13, and 15, respectively. As shown in Figure 2A, there were very low fluorescence intensities of CuNCs when the length of poly(AT-TA) in the template dsDNA was lower than or equal to 7. The reason is that the synthesis efficiency of CuNCs was low when using template dsDNA with short poly(AT-TA). When the length of poly(AT-TA) increased from 10 to 15, the fluorescence intensities increased gradually. The results demonstrated that the length of poly(AT-TA) in the template dsDNA was proportional to the fluorescence intensities of CuNCs. Then, the probe DNA reacted with 9000 nM BRCA1 gene and the fluorescence intensities were measured by the fluorescence spectrophotometer. The subtractive difference ($F_{\text{blank}} - F_{\text{BRCA1}}$) and the ratio ($F_{\text{BRCA1}}/F_{\text{blank}}$) of the fluorescence intensities between the

signals produced by the blank and the BRCA1 gene are shown in Figure 2B. The values of $F_{\text{blank}} - F_{\text{BRCA1}}$ were 9, 17, 23, 41, 228, 1020, 487, and 474 using the template dsDNA with 1, 2, 3, 5, 7, 10, 13, and 15 poly(AT-TA), respectively. The template dsDNA with 10 poly(AT-TA) produced the highest value of $F_{\text{blank}} - F_{\text{BRCA1}}$. The values of $F_{\text{BRCA1}}/F_{\text{blank}}$ were 0.632, 0.355, 0.401, 0.304, 0.155, 0.240, 0.651 and 0.696 using the template dsDNA with 1, 2, 3, 5, 7, 10, 13, and 15 poly(AT-TA), respectively. The ratio of $F_{\text{BRCA1}}/F_{\text{blank}}$ for DNA7 was the smallest. The ratio of $F_{\text{BRCA1}}/F_{\text{blank}}$ for DNA10 was a little higher than that of DNA7, while the change of the fluorescence intensity ($F_{\text{blank}} - F_{\text{BRCA1}}$) for DNA10 was about 4.5 times higher than that for DNA7. Considering the potential of the assay method for point-of-care using UV light and a phone application, the larger change of the fluorescence intensity ($F_{\text{blank}} - F_{\text{BRCA1}}$) could make it easier to observe the fluorescent red emission change of CuNCs. Therefore, DNA10 was selected as the optimal sequence for probe DNA.

Characterization and stability of DNA-templated CuNCs

Poly(AT-TA) dsDNA acted as an efficient template to support the formation of CuNCs.^{34,35} The CuNCs were accumulated in the major groove of the dsDNA during the process of synthesis and thus, DNA was present in the CuNCs. The fluorescence excitation and emission spectra of CuNCs were investigated by the fluorescence spectrophotometer. Ultraviolet visible absorption spectra were measured on UV-Vis spectrophotometer. As shown in Figure 3A, the CuNCs were excited at about 361 nm (curve a), emitted at 580 nm (curve b) and exhibited a distinct absorption peak at 340 nm (curve c). Thus, the excitation wavelength and emission wavelength were set at 340 nm and emitted at 580 nm for the subsequent experiment, respectively. The shelf life of CuNCs was

then investigated by recording the fluorescence spectrum at different times. It is noted from Figure 3B that the fluorescence intensity of CuNCs decreased by about 4.7% after 30 min, which was consistent with the result reported by Mukherjee and co-workers.³⁶ Therefore, the shelf life of CuNCs was 30 min. The morphology of CuNCs was characterized by HRTEM. The results shown in Figure 3C demonstrated that the freshly prepared CuNCs exhibited a uniform spherical shape with a diameter of 5 nm, which was consistent with our previous work.³⁷ CuNCs could be easily oxidized by gaseous or dissolved oxygen, resulting in their low catalytic activity and poor stability.³⁸ Therefore, it was necessary to investigate the nanostructure stability of CuNCs. The prepared CuNCs were stored at 4 °C for 7 days, and the morphology of CuNCs was characterized by HRTEM. As shown in Figure 3D, the images indicated that the formed CuNCs were spherical in shape, and their average sizes were about 5 nm. After 7 days, the nanostructure of CuNCs was almost unchanged with a comparison to the freshly prepared CuNCs, indicating good nanostructure stability.

Feasibility of the fluorescent sensor towards BRCA1 gene assay

The application of the developed fluorescent sensor for the detection of BRCA1 gene was investigated. The fluorescence intensities of the blank and the detection system with 9000 nM BRCA1 gene were measured by the fluorescence spectrophotometer. The emission pictures of the detection system under the UV lamp excitation were obtained by a smartphone. It is noted from the inset of Figure 4a that there was a strong red emission for the blank, while the system in the presence of BRCA1 gene showed weak red emission. The reason is that BRCA1 gene

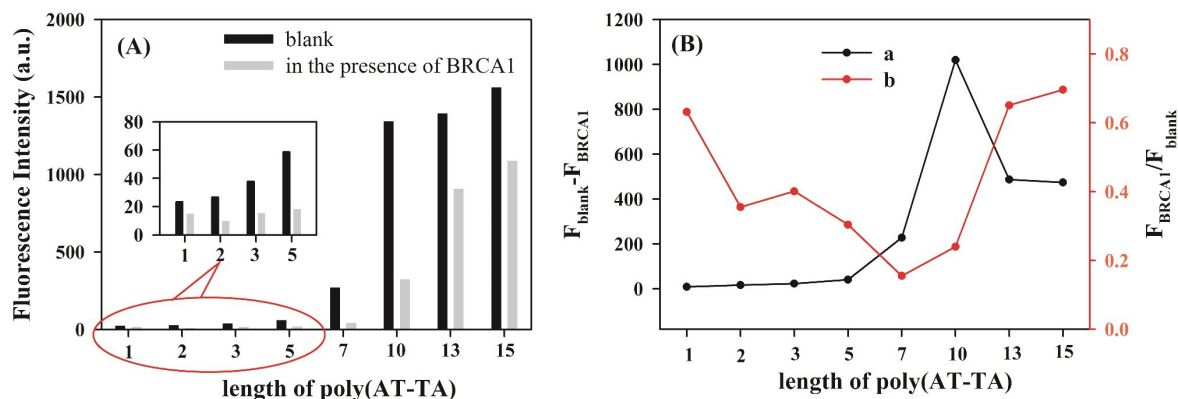


Figure 2. (A) The effect of the length of poly(AT-TA) in the template dsDNA on the fluorescence intensity; inset: a zoomed-in view of the data; (B) the relationship between $F_{\text{blank}} - F_{\text{BRCA1}}$ (a) or $F_{\text{BRCA1}}/F_{\text{blank}}$ (b) and the length of poly(AT-TA) in the template dsDNA; F_{blank} and F_{BRCA1} are the fluorescence intensities without and with the presence of T-DNA, respectively.

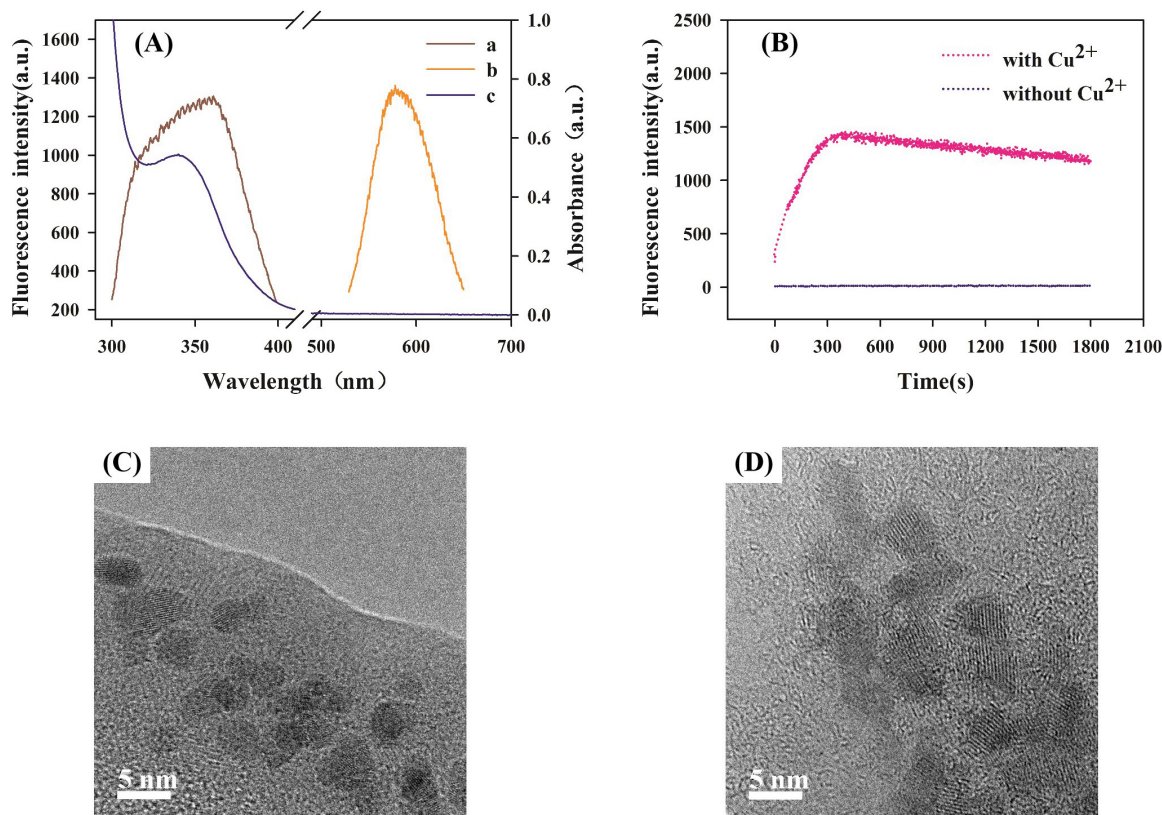


Figure 3. (A) The fluorescence excitation (a), emission (b) and UV-Vis absorption (c) spectra of CuNCs using DNA10 as the template DNA. (B) Temporal change in fluorescence intensity at 580 nm with Cu²⁺ and without Cu²⁺; TEM images of the freshly prepared CuNCs (C) and the CuNCs stored at 4 °C for 7 days (D).

was in close proximity to the dsDNA and hybridized with 3' protruding termini of the dsDNA. This increased the steric resistance and decreased the synthetic efficiency of CuNCs. By integrating a UV lamp and a mobile phone, the red emission of the reaction system could be recorded in the form of pictures. The fluorescence color change could be measured by an application that runs on an inexpensive smartphone internal processor, providing an excellent prospective application in point-of-care for monitoring the breast cancer risk. The fluorescence spectra of the detection systems are also shown in Figure 4a. The fluorescence intensities with emission at 580 nm were 1342 and 307 for the blank and the BRCA1 gene detection, respectively, which were consistent with the above red emission pictures. All the results demonstrated that the assay method was feasible to detect BRCA1 gene.

Optimization of the reaction parameters

Several reaction parameters were optimized, including the concentration of the template dsDNA (C_{dsDNA}), the concentration of Cu²⁺ ($C_{\text{Cu}^{2+}}$) and the concentration of AA (C_{AA}). DNA10 was first self-hybridized to form the poly(AT-TA) dsDNA and then used as a template for

synthesizing the CuNCs. The fluorescence of the reaction system without BRCA1 gene was measured. The effect of C_{dsDNA} on the fluorescence signal was investigated at first. It is noted from Figure 4b that the fluorescence intensity increased gradually when the C_{dsDNA} increased from 0.25 to 2 μM and then reached a plateau when the C_{dsDNA} was equal to or larger than 2 μM . The results indicated that 2 μM of the dsDNA was enough for this detection system and selected as the optimized C_{dsDNA} . Then, the effect of $C_{\text{Cu}^{2+}}$ on the response signal was investigated since it influenced the yield of CuNCs. The results are presented in Figure 4c. The fluorescence intensity increased at first and then decreased with the increase of $C_{\text{Cu}^{2+}}$. The highest fluorescent signal was obtained when $C_{\text{Cu}^{2+}}$ was 0.3 mM, which was chosen as the optimum $C_{\text{Cu}^{2+}}$. AA was used to reduce copper ions and its concentration (C_{AA}) was another important parameter. It is observed from Figure 4d that the response intensity increased when C_{AA} increased from 0.1 to 2 mM but decreased with the further increase of C_{AA} . The possible reason is that 2 mM AA was enough to reduce all the Cu²⁺ in this detection system. Therefore, 2 mM was selected as the optimized C_{AA} in the detection system.

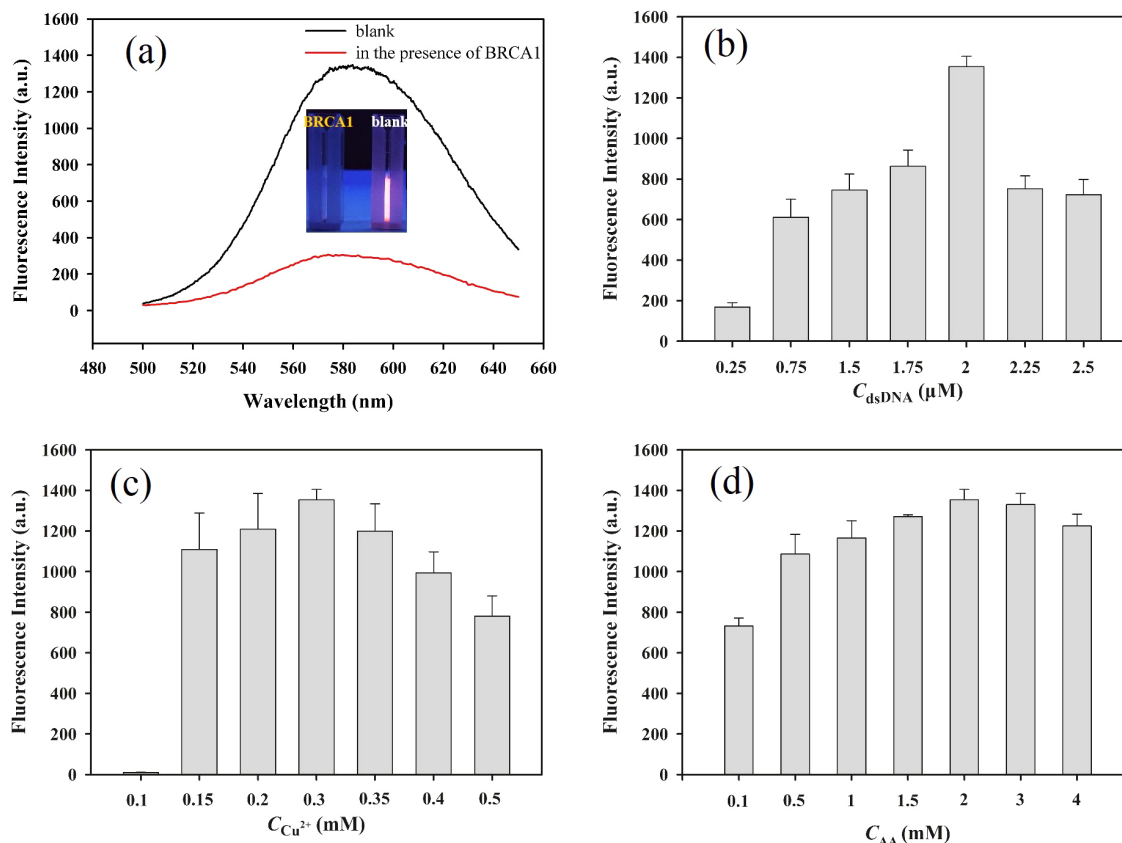


Figure 4. (a) The fluorescence spectra of the system without BRCA1 and with BRCA1; inset: the photographs of the reaction system in the presence (left) and absence (right) of BRCA1 gene under the UV lamp (365 nm); the effect of C_{dsDNA} (b), $C_{Cu^{2+}}$ (c) and C_{AA} (d) on the fluorescence intensity.

Analytical performance of the fluorescence sensor for BRCA1 assay

Under the optimized conditions, a series of BRCA1 gene with different concentrations were detected by the developed fluorescence sensor as shown in the fluorescent spectra in Figure 5a. It is noted that when the concentration of BRCA1 increased from 0 to 9000 nM, the fluorescence intensity of the detection system decreased gradually. Figure 5b showed that the linear range for BRCA1 gene assay was 2-600 nM and the linear equation was fluorescence intensity = $-0.43 \times C_{BRCA1} + 1289$ (square of the correlation coefficient (R^2) = 0.9926). The LOD is the minimum detectable concentration, which can be significantly distinguished from the background fluorescence of probe CuNCs.³⁹ In this work, the lowest detectable concentration of BRCA1 gene was 2 nM, which was the LOD of our method. The assay performance of the developed fluorescent sensor was compared with other sensors reported for BRCA1 gene assay. Table 1 briefly presents the assay performance of the previously reported biosensors for BRCA1 gene detection. It is noted that the sensor based on CuNCs developed in this work exhibited a lower LOD in comparison with most of the sensors

based on other nanomaterials. The LOD obtained by the sensors based on metal nanoclusters prepared by Li *et al.*⁴⁰ was much lower than that of the CuNCs-based sensor developed in this work. The possible reason is that they used enzyme for the signal amplification to achieve higher sensitivity. The fluorescent sensor developed in this work exhibited a wide dynamic range, which was comparable to the performances obtained by other reported sensors. More importantly, the sensing material used in this work was CuNCs, which could be simply synthesized without the need to incorporate additional labels (for amplification step).

Selectivity investigation

Selectivity is one of the important criteria to judge the performance of the sensor, which means being able to distinguish the analyte from other interferent species in the sample. Several DNA strands with mismatched bases were used as interferents for the selectivity experiment. The results are shown in Figure 6. It is noted that the fluorescent intensity for T-DNA (2000 nM) was about 73.8, 62.0, 59.8, and 55.9% of those for Sm-DNA, Twm-DNA, Thm-DNA and N-DNA, respectively. The change of the fluorescence

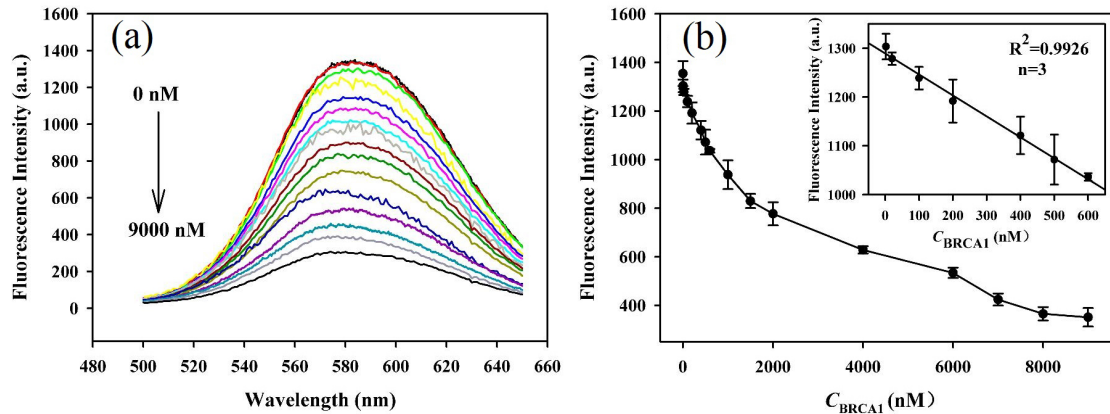


Figure 5. (a) The fluorescence spectra of the sensor for the detection of BRCA1 gene with different concentrations: 0, 2, 20, 100, 200, 400, 500, 600, 1000, 1500, 2000, 4000, 6000, 7000, 8000, 9000 nM. (b) Plots of the fluorescence intensities as a function of concentrations of BRCA1 gene (C_{BRCA1}). Inset: linear calibration plot for BRCA1 gene. Error bars were obtained from three parallel experiments.

Table 1. Comparison of the assay performance of different sensors for DNA detection

Sensing element	Technique	Target	Linear range / nM	LOD / nM	Reference
Molecular beacon	fluorescence	DNA	200-5000	70	17
AgNCs	fluorescence	BRCA1	1-1000	1	39
CuNCs			0.0005-0.1	0.00054	
AuNCs	fluorescence	DNA	0-1	0.16241	40
AgNCs			0-2	0.07824	
AuNPs and carbon dots	fluorescence	BRCA1	4-120	2.1	41
AgNCs	luminescence	mutant DNA	–	53	42
AgNCs	luminescence	BRCA1	10-80	9	43
Cyclometallated iridium(III) complex	luminescence	gene	0-500	50	44
γ PNA arrays	fluorescence	BRCA1	0-2000	5.97	45
Perylene-labeled DNA probes	fluorescence	BRCA1	–	100	46
Carbon nanotubes	electrochemistry	BRCA1	161-1937	378.5	6
Monolithic silicon	fluorescence	BRCA1	1-500	0.9	47
DNA	electrochemistry	BRCA1	0.1-10	0.05	48
CuNCs	fluorescence	BRCA1	2-600	2	this work

LOD: limit of detection; DNA: deoxyribonucleic acid; AgNCs: silver nanoclusters; AuNCs: gold nanoclusters; BRCA1: breast cancer susceptibility gene 1; AuNPs: gold nanoparticles; γ PNA: gamma peptide nucleic acids; CuNCs: copper nanoclusters.

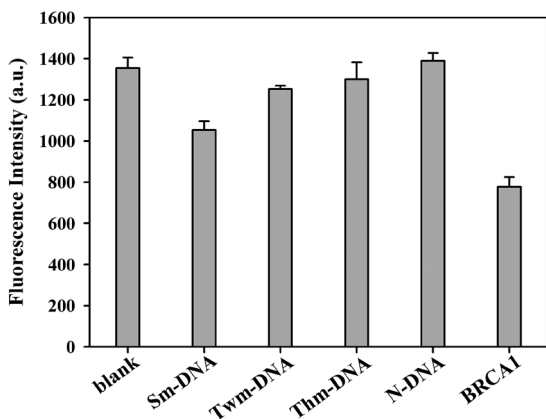


Figure 6. Selectivity of the sensing strategy for the BRCA1 gene assay. Fluorescence intensities of the detection system in the presence of BRCA1 gene, Sm-DNA, Twm-DNA, Thm-DNA and N-DNA, respectively. The concentration of the mismatched DNA was fixed at 2000 nM.

intensities decreased as the number of mismatched bases rose. The sensing method had significant selectivity to distinguish the full-matched and mismatched. Moreover, the selectivity of the CuNCs-based sensor developed in this work was comparable with that of other sensors based on different nanomaterials.^{39,41,43,49} In view of these results, the proposed fluorescent method exhibited a satisfactory selectivity for BRCA1 gene assay.

Spike recovery

Another important performance requirement of the sensor is spike recovery. The BRCA1 gene is easily encountered in human serum.⁵⁰ For the general population at risk of breast cancer, serum is a preferable choice of

body fluid for molecular detection. The reason is that serum is readily accessible in all individuals from a peripheral blood sample, and is enriched for tumor DNA in cancer patients.⁵¹ The concentration of the BRCA1 gene in human samples is at pM level.⁵² Therefore, the 20-fold diluted fetal bovine serum was used as the complex sample for recovery experiments. A known concentration of BRCA1 gene was added to the serum sample to test whether the fluorescence response is the same as that expected from the calibration curve. The recoveries for the serum samples spiked with 100, 300 and 600 nM BRCA1 gene were 98, 100 and 93%, respectively. These results indicated that the fluorescent sensor based on CuNCs provided a reliable and practical platform for the detection of BRCA1 gene in real sample.

More importantly, based on the work done by our group in the microfluidic colorimetric detection,⁵³⁻⁵⁶ the fluorescent red emission of CuNCs in this work could be recorded as measured color values in the red, green, blue (RGB) color system. In further work, the fluorescent sensor would be transferred to a microfluidic chip for point-of-care testing, offering high sample throughput, portability, low-cost detection and no requirement for the fluorescence spectrometer.

Conclusions

In this work, a rapid, simple, selective, and cost-effective fluorescent sensing platform has been developed for the sensitive detection of BRCA1 gene. The dsDNA with 10 poly(AT-TA) complimentary base pairs was used to template the formation of CuNCs with high fluorescence and good stability. BRCA1 gene was in close proximity to the DNA probe, resulting in a big steric resistance and decreasing the synthetic efficiency of CuNCs. As a result, the yield of CuNCs decreased and a weak fluorescence was obtained. The fluorescence signal was inversely related to the concentration of BRCA1 gene. The linear range was 2-600 nM and the LOD for BRCA1 gene assay was 2 nM. More importantly, the developed method exhibited good selectivity towards single base mismatched DNA, indicating a promising prospect for the genetic mutation detection. In addition, the assay method showed satisfactory recoveries to detect BRCA1 gene in the diluted serum.

Acknowledgments

The authors are grateful to the financial support from National Innovation Training Program for college students (grant No. 202110530018) and the National Natural Science Foundation of China (grant No. 21804114).

Author Contributions

J. H. was responsible for carry out the experiments; T. Y. and Z. L. for the manuscript writing and edition; B. X. for the data analysis; P. Y. for the funding acquisition, project administration and supervision.

References

1. Ferlay, J.; Colombet, M.; Soerjomataram, I.; Mathers, C.; Parkin, D. M.; Piñeros, M.; Znaor, A.; Bray, F.; *Int. J. Cancer* **2019**, *144*, 1941. [Crossref]
2. Tan, D. S. P.; Marchiò, C.; Reis-Filho, J. S.; *J. Clin. Pathol.* **2008**, *61*, 1073. [Crossref]
3. Larsen, M. J.; Thomassen, M.; Gerdes, A. M.; Kruse, T. A.; *Breast Cancer: Basic Clin. Res.* **2014**, *8*, 145. [Crossref]
4. Valencia, O. M.; Samuel, S. E.; Viscusi, R. K.; Riall, T. S.; Neumayer, L. A.; Aziz, H.; *JAMA Surg.* **2017**, *152*, 589. [Crossref]
5. Ford, D.; Easton, D. F.; Bishop, D. T.; Narod, S. A.; Goldgar, D. E.; *Lancet* **1994**, *343*, 692. [Crossref]
6. Li, C.-z.; Karadeniz, H.; Canavar, E.; Erdem, A.; *Electrochim. Acta* **2012**, *82*, 137. [Crossref]
7. Park, K.; Kim, M. K.; Lee, T.; Hong, J.; Kim, H.-K.; Ahn, S.; Lee, Y.-J.; Kim, J.; Lee, S. W.; Lee, J. W.; Lee, W.; Chun, S.; Son, B. H.; Jung, K. H.; Kim, Y. M.; Min, W. K.; Ahn, S. H.; *J. Clin. Lab. Anal.* **2020**, *34*, e23524. [Crossref]
8. Minucci, A.; Bonis, M. D.; Paolis, E. D.; Gentile, L.; Santonocito, C.; Concolino, P.; Mignone, F.; Capoluongo, E.; *Mol. Diagn. Ther.* **2017**, *21*, 217. [Crossref]
9. Liang, D.; You, W.; Yu, Y.; Geng, Y.; Lv, F.; Zhang, B.; *RSC Adv.* **2015**, *5*, 27571. [Crossref]
10. Rashid, T.-R.; Phan, D.-T.; Chung, G.-S.; *Sens. Actuators, B* **2014**, *193*, 869. [Crossref]
11. Zou, F.; Ruan, Q.; Lin, X.; Zhang, M.; Song, Y.; Zhou, L.; Zhu, Z.; Lin, S.; Wang, W.; Yang, C. J.; *Biosens. Bioelectron.* **2019**, *126*, 551. [Crossref]
12. Bansal, J.; Singh, I.; Bhatnagar, P. K.; Mathur, P. C.; *J. Biosci. Bioeng.* **2013**, *115*, 438. [Crossref]
13. Li, F.; Mahon, A. R.; Barnes, M. A.; Feder, J.; Lodge, D. M.; Hwang, C.-T.; Schafer, R.; Ruggiero, S. T.; Tanner, C. E.; *PLoS One* **2011**, *6*, e29224. [Crossref]
14. Zhang, Q.; Tian, Y.; Liang, Z.; Wang, Z.; Xu, S.; Ma, Q.; *Anal. Chem.* **2021**, *93*, 3308. [Crossref]
15. Hossain, M. B.; Islam, M. M.; Abdulrazak, L. F.; Rana, M. M.; Akib, T. B. A.; Hassan, M.; *Photonic Sens.* **2020**, *10*, 67. [Crossref]
16. Wei, W.; Gao, C.; Xiong, Y.; Zhang, Y.; Liu, S.; Pu, Y.; *Talanta* **2015**, *131*, 342. [Crossref]
17. Culha, M.; Stokes, D. L.; Griffin, G. D.; Vo-Dinh, T.; *Biosens. Bioelectron.* **2004**, *19*, 1007. [Crossref]
18. Rasheed, P. A.; Sandhyarani, N.; *Analyst* **2015**, *140*, 2713. [Crossref]

19. Borghei, Y.-S.; Hosseini, M.; Ganjali, M. R.; Hosseinkhani, S.; *J. Pharm. Biomed. Anal.* **2018**, *152*, 81. [Crossref]
20. Borghei, Y.-S.; Hosseini, M.; Ganjali, M. R.; Ju, H.; *Mat. Sci. Eng. C* **2019**, *97*, 406. [Crossref]
21. Qing, Z.; He, X.; He, D.; Wang, K.; Xu, F.; Qing, T.; Yang, X.; *Angew. Chem., Int. Ed.* **2013**, *52*, 9719. [Crossref]
22. Zhou, Z.; Du, Y.; Dong, S.; *Anal. Chem.* **2011**, *83*, 5122. [Crossref]
23. Chen, M.; Xiang, X.; Wu, K.; He, H.; Chen, H.; Ma, C.; *Sensors* **2017**, *17*, 2684. [Crossref]
24. Liu, R.; Wang, C.; Hu, J.; Su, Y.; Lv, Y.; *TrAC, Trends Anal. Chem.* **2018**, *105*, 436. [Crossref]
25. Qing, Z.; Zhu, L.; Yang, S.; Cao, Z.; He, X.; Wang, K.; Yang, R.; *Biosens. Bioelectron.* **2016**, *78*, 471. [Crossref]
26. Ji, D.; Du, Y.; Meng, H.; Zhang, L.; Huang, Z.; Hu, Y.; Li, J.; Yu, F.; Li, Z.; *Sens. Actuators, B* **2018**, *256*, 512. [Crossref]
27. Ge, J.; Dong, Z.-Z.; Bai, D.-M.; Zhang, L.; Hu, Y.-L.; Ji, D.-Y.; Li, Z.-H.; *New J. Chem.* **2017**, *41*, 9718. [Crossref]
28. Chen, X.; Yang, D.; Tang, Y.; Miao, P.; *Analyst* **2018**, *143*, 1685. [Crossref]
29. Cai, Q.; Ge, J.; Xu, H.; Zhang, L.; Hu, Y.; Huang, Z.; Li, Z.; *Anal. Methods* **2017**, *9*, 2710. [Crossref]
30. Song, C.; Hong, W.; Zhang, X.; Lu, Y.; *Analyst* **2018**, *143*, 1829. [Crossref]
31. Qing, T.; Qing, Z.; Mao, Z.; He, X.; Xu, F.; Wen, L.; He, D.; Shi, H.; Wang, K.; *RSC Adv.* **2014**, *4*, 61092. [Crossref]
32. Wang, X.; Long, C.; Jiang, Z.; Qing, T.; Zhang, K.; Zhang, P.; Feng, B.; *Anal. Methods* **2019**, *11*, 4580. [Crossref]
33. Mohan, S.; Nigam, P.; Kundu, S.; Prakash, R.; *Analyst* **2010**, *135*, 2887. [Crossref]
34. Rotaru, A.; Dutta, S.; Jentzsch, E.; Gothelf, K.; Mokhir, A.; *Angew. Chem., Int. Ed.* **2010**, *49*, 5665. [Crossref]
35. Li, J.; Zhu, J. J.; Xu, K.; *TrAC, Trends Anal. Chem.* **2014**, *58*, 90. [Crossref]
36. Shekhar, S.; Mahato, P.; Yadav, R.; Verma, S. D.; Mukherjee, S.; *ACS Sustainable Chem. Eng.* **2022**, *10*, 1379. [Crossref]
37. Lei, T.; Huang, T.; Wang, T.; Yu, P.; Qing, T.; Nie, P.; *New J. Chem.* **2020**, *44*, 17296. [Crossref]
38. Chen, S.; Li, Z.; Huang, Z.; Jia, Q.; *Sens. Actuators, B* **2021**, *332*, 129522. [Crossref]
39. Teng, Y.; Tateishi-Karimata, H.; Tsuruoka, T.; Sugimoto, N.; *Molecules* **2018**, *23*, 2889. [Crossref]
40. Tao, Y.; Yi, K.; Wang, H.; Li, K.; Li, M.; *Sens. Actuators, B* **2022**, *361*, 131711. [Crossref]
41. Zhong, D.; Yang, K.; Wang, Y.; Yang, X.; *Talanta* **2017**, *175*, 217. [Crossref]
42. Wang, M.; Wang, W.; Liu, C.; Liu, J.; Kang, T.-S.; Leung, C.-H.; Ma, D.-L.; *Mater. Chem. Front.* **2017**, *1*, 128. [Crossref]
43. Wang, F.; Sharon, E.; Albada, H. B.; Willner, I.; *ACS Nano* **2014**, *8*, 11666. [Crossref]
44. He, H.-Z.; Chan, D. S.-H.; Leung, C.-H.; Ma, D.-L.; *Chem. Commun.* **2012**, *48*, 9462. [Crossref]
45. Dong, B.; Nie, K.; Shi, H.; Chao, L.; Ma, M.; Gao, F.; Liang, B.; Chen, W.; Long, M.; Liu, Z.; *Biosens. Bioelectron.* **2019**, *136*, 1. [Crossref]
46. Kashida, H.; Kondo, N.; Sekiguchi, K.; Asanuma, H.; *Chem. Commun.* **2011**, *47*, 6404. [Crossref]
47. Mavrogiannopoulou, E.; Petrou, P. S.; Kakabakos, S. E.; Misikakos, K.; *Biosens. Bioelectron.* **2009**, *24*, 1341. [Crossref]
48. Xu, H.; Wang, L.; Ye, H.; Yu, L.; Zhu, X.; Lin, Z.; Wu, G.; Li, X.; Liu, X.; Chen, G.; *Chem. Commun.* **2012**, *48*, 6390. [Crossref]
49. Borghei, Y. S.; Hosseini, M.; Ganjali, M. R.; *Methods Appl. Fluoresc.* **2017**, *6*, 015001. [Crossref]
50. Jing, F.; Jun, L.; Yong, Z.; Wang, Y.; Fei, X.; Zhang, J.; Hu, L.; *Oncology* **2008**, *75*, 60. [Crossref]
51. Chang, H.-W.; Lee, S.-M.; Goodman, S. N.; Singer, G.; Cho, S. K. R.; Sokoll, L. J.; Montz, F. J.; Roden, R.; Zhang, Z.; Chan, D. W.; Kurman, R. J.; Shih, I. M.; *JNCI, J. Natl. Cancer Inst.* **2002**, *94*, 1697. [Crossref]
52. Hui, N.; Sun, X.; Niu, S.; Luo, X.; *ACS Appl. Mater. Interfaces* **2017**, *9*, 2914. [Crossref]
53. Nie, B.; Zhao, S.; Deng, M.; Yu, P.; Yang, Y.; Lei, W.; Yin, L.; *J. Braz. Chem. Soc.* **2021**, *32*, 599. [Crossref]
54. Yu, P.; Deng, M.; Yang, Y.; Nie, B.; Zhao, S.; *Sensors* **2020**, *20*, 4118. [Crossref]
55. Yu, P.; Deng, M.; Yang, Y.; *Sensors* **2019**, *19*, 4082. [Crossref]
56. Deng, M.; Liao, C.; Wang, X.; Chen, S.; Qi, F.; Zhao, X.; Yu, P.; *Can. J. Chem.* **2019**, *97*, 373. [Crossref]

Submitted: June 2, 2022

Published online: December 12, 2022

